Deposition and diffusion of plasma sputtered platinum nanoparticles in porous anodic alumina oxide

Sujuan Wu, Pascal Brault, Cong Wang

Deposition and diffusion of plasma sputtered platinum nanoparticles in porous anodic alumina oxide.

Sujuan Wu[1,2], Pascal Brault[2*], Cong Wang[1]

[1]School of Physics and Nuclear Energy Engineering, Beihang University, Beijing 100191, China

[2]GREMI UMR 6606 CNRS-Université d'Orléans, 14, rue d'Issoudun BP 6744, F-45067 ORLEANS Cedex 2, France

Abstract

Plasma sputtering deposition of Platinum thin films is studied on porous anodic aluminum oxide (AAO) template. The size effect of AAO cylindrical pores is shown to influence the diffusion of atoms in the porous layer. The resulting maximum reached depth of platinum varied from 2 μm to 20 μm, and the density on the surface is lowered from 23 $\mu g.cm^{-2}$ to 5 $\mu g.cm^{-2}$ as the pore diameter increased from 40 nm to 320 nm. The pore diameter is decreasing as Pt is deposited. Sputtered Pt is observed to grow as clusters on the surface and along the pore walls.

Keywords

Anodic aluminum oxide; Sputtering; Platinum; Anomalous diffusion; RBS

(*) Corresponding author: Pascal.Brault@univ-orleans.fr

Introduction

Plasma sputtering deposition of precious metals on porous substrate, such as porous materials, membranes with nanochannels and nanoarrays, is important in physical process and applications [1-4]. The advantage of controlling growth and depth concentration profiles is particularly useful in the field of catalysis, which is helpful to increasing the efficiency and reducing the waste of noble metal catalyst [5-6]. Earlier experiments [7-9] have shown great promise for this technique and the deposition into porous materials, but a clear description of Pt penetration into the nanochannels membranes and resulting concentration profiles remains to be established. In order to obtain more detailed information of Pt deposition in nanochannels, a porous anodic alumina oxide (AAO) membrane has been used as substrate.

AAO membrane is a typical self-ordered nanochannel material formed by anodization of Al in an appropriate acid solution. The structure of AAO is a close-packed array of columnar cells, each containing a central cylindrical pore of which the diameter and interval can be controlled by changing the forming conditions. Normally, the pore diameter can be adjusted from 25 to 350 nm and aspect ratio can be changed by controlling the anodizing time [10-12]. It has already been used as hard-template to control the growth of nanotubes, nanowires and nanodots using chemical methods. Up to now, the Pt[13,14], Si[15], Bi[16], PbO[17], SnO_2[18], NiO[19], $LiMn_2O_4$[20] nanowires and nanotubes have already been successfully prepared. Unfortunately, controlled growth of nanowires in the template by plasma sputtering technology is difficult to achieve, due to the isotropic distribution of the sputtered atoms reaching the template. Herein, to study the distribution of sputtered particles in the template and to control the distribution of the nanoparticles, is not only helpful for studying the diffusion process, it is also advantageous for controlling the growth of nanostructures.

Since the sputtered platinum atoms are deposited on the surface and penetrate into the pore of the AAO template, the morphology of the surface and the pore size of the template may have a drastic impact on the deposition and diffusion process. The goal of the experiments is to characterize the morphology and to determine the depth-density

profiles of Pt coated templates having different cylindrical pore diameter.

Experimental

A low pressure, high frequency (VHF) inductive plasma sputtering system has been applied as displayed in Fig 1. An argon plasma is created in the stainless steel deposition chamber by using an external planar antenna (TCP) at 100 W input power and an argon pressure of $2.4*10^{-3}$ mbar. The excitation antenna is powered by a radiofrequency generator operating 13.56 MHz. The electrodes are placed on a movable/rotating grounded substrate holder in front of the sputtering target with a target-substrate distance of 8 cm. A base pressure of $P_0 = 2.7*10^{-7}$ mbar is achieved using a primary/turbomolecular pump combination. The argon flow is fixed to 5 sccm using a mass flow meter.

The coated Pt AAO templates were analyzed by high resolution scanning electron microscopy (SEM) (ZEISS) to determine pore size and evolution of the porosity at the surface. The line scan profile on the EDX (energy dispersive X-ray spectrometry) was carried out to observe the presence of platinum along the pores. Rutherford Backscattering Spectroscopy), with a Van de Graaf accelerator (CEMHTI-CNRS, Orleans, France) using a 2 MeV $^4He^+$ ion beam, was used to measure the total Pt content and to quantify Pt penetration into pores.

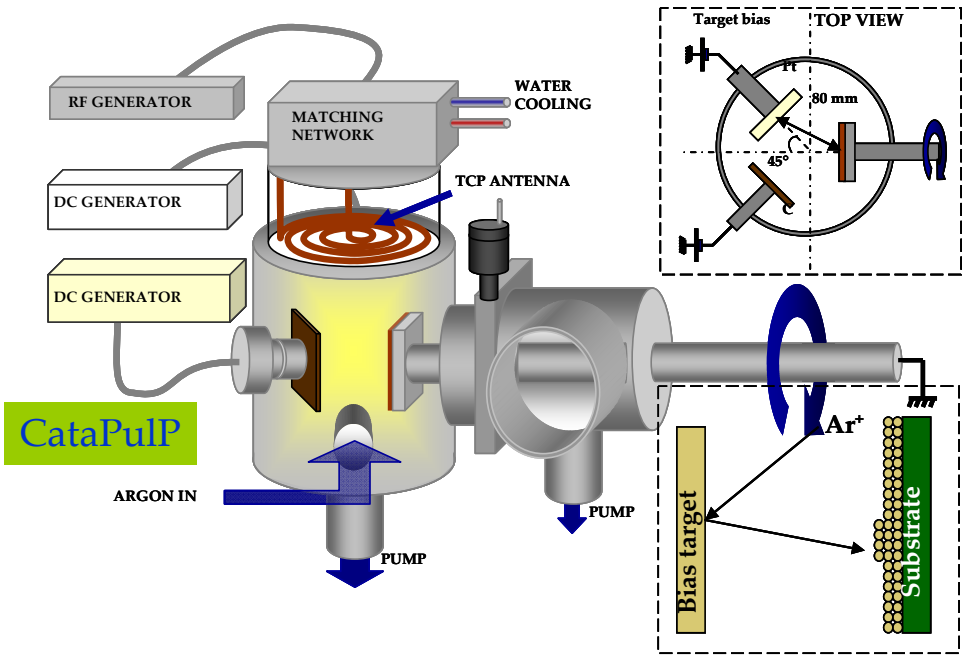

Figure 1: Schematic of the plasma sputtering reactor called “CataPulP”.

Results and discussion

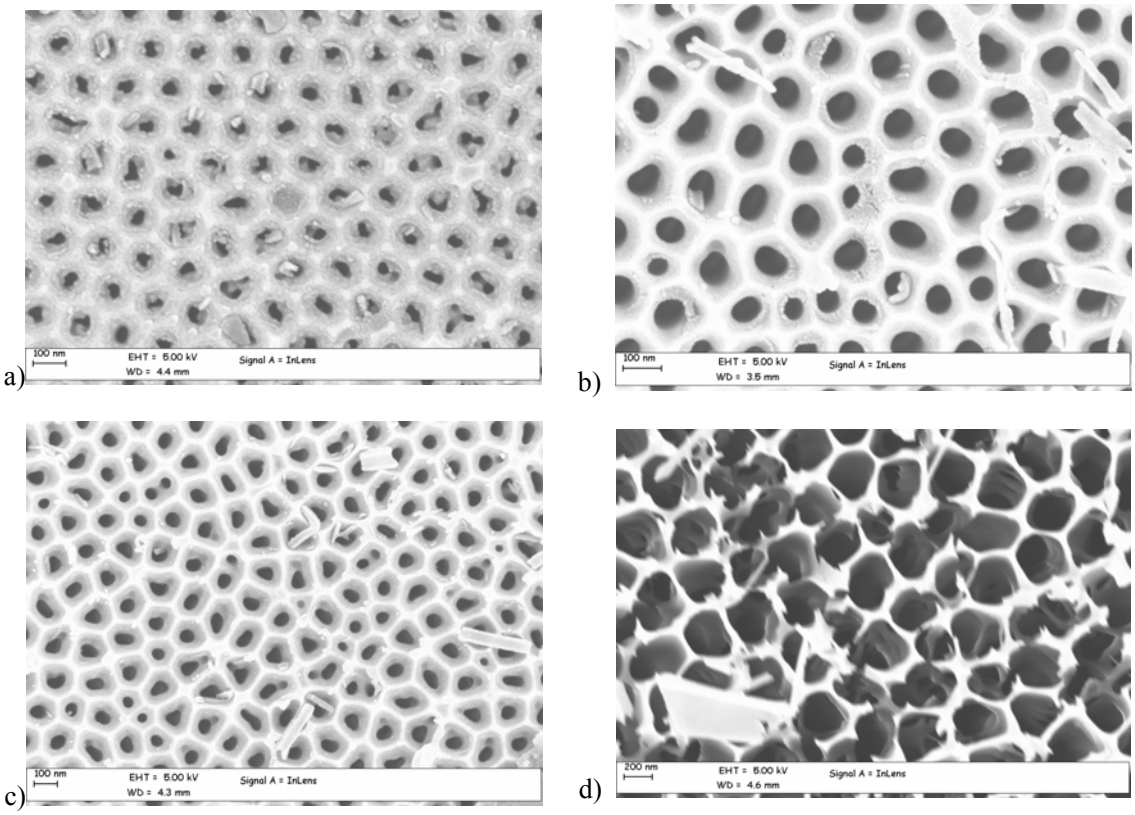

Figure 2: The morphology of AAO templates with different average pore sizes (a) 40-60 nm (b) 80-100 nm (c) 90-110 nm (d) 270-320 nm. A low amount of Pt has been deposited for good imaging by SEM.

SEM micrographs of the AAO template are shown in figure 2. The average diameters of the AAO pores are varied from 40 to 320 nm (figure 2(a) to figure 2(d)). The templates were exposed 3 min to the sputtering Pt flux. Even though it is a short time deposition, the reducing of pore sizes still can be observed in figure 2 (a) and figure 2 (b).

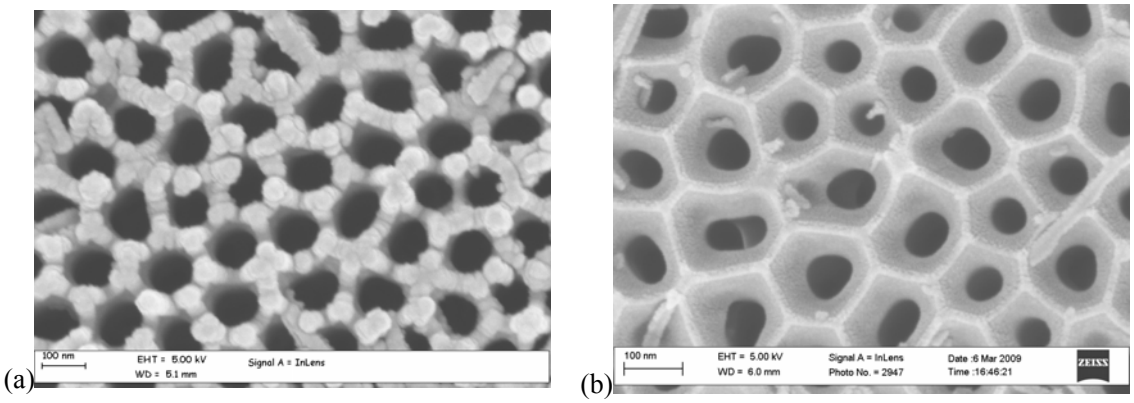

(c) 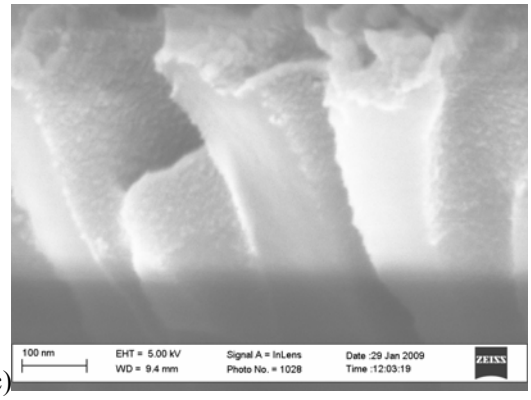

Figure 3: Various Pt coated AAO showing the structure of the deposit on and in the pores. (a) Pt deposited on smooth AAO surface (b) Pt deposited on the AAO surface which looks like a funneled pore surrounded the holes (c) cross section view showing Pt diffusion along inner pore walls.

Figure 3 displays some selected SEM views of the Pt coated AAO. After Pt deposition, the Pt atoms are stacked on the smooth surfaces of the AAO (Figure 3 (a)). Kai-Tze Huang *et al* also have reported that the AAO surface is used to provide the nucleation and growth sites for the formation of Pt nanorods [21]. In figure 3 (b), the surface of the templates looks like a funneled pore surrounding the vacant space. When the templates were exposed to the flux of sputtered Pt, Pt atoms were driven to travel across this surface and fall into the holes. A zoom on the cross section shows that the pore walls are coated by Pt clusters with a size of 10 nm (figure 3(c)), implying that Pt atoms are subject to transport/diffusion/adsorption on the inner walls and cluster growth. The rate of diffusion and absorption on the AAO surface are not consistent with the sputtering rate. Usually it is higher than the diffusion and absorption rate that caused most of Pt particles concentrated on the surface.

(a) 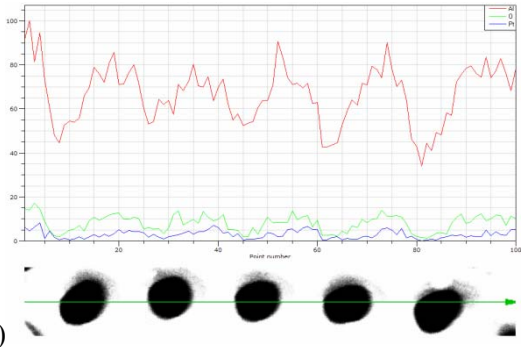

(b) 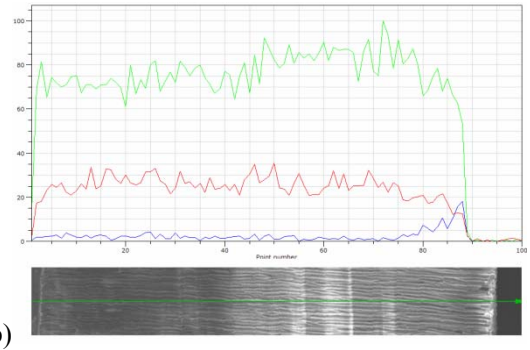

Figure 4: EDX scanning of Pt, Al, O elements (a) line scan crossing pores along the surface (b) line scan along a pore in a cross section view.

Figure 4(a) is displaying the Al, O and Pt concentrations along the selected straight line crossing some pores drawn below the diagram in Figure 4(a). On the other hand, Figure 4(b) reports the Pt, Al, O concentration profiles along the inner surface of a pore. The amounts of Pt and Al are obviously dropped simultaneously at the position of the holes (Figure 4(a)). The distribution of Pt in the pores is visualized in Figure 4(b), the Pt amount is decreasing as increasing the depth. The particle flux delivered by the plasma sputtering cannot be absorbed directly by the porous AAO template. Part of Pt particles is deposited on the surface between pores and part of the Pt is diffusing into the porous and adsorbed on the inner walls.

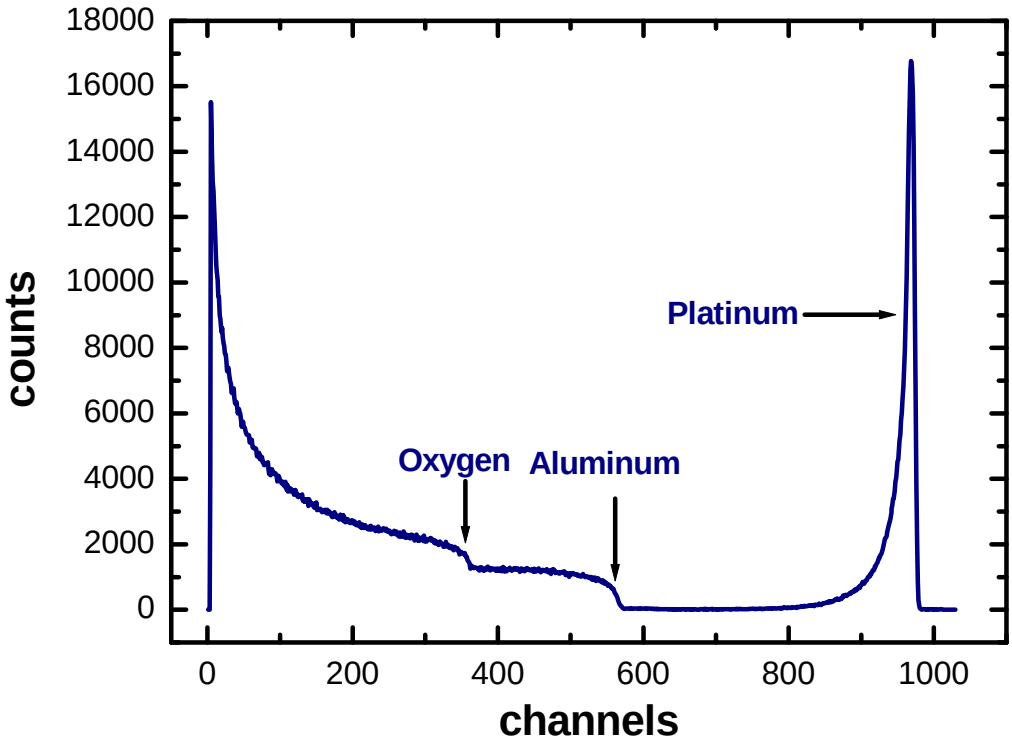

Figure 5: The RBS spectra of the Pt deposited on the AAO, the average pore size is 80nm and deposition time is 5min.

RBS measurements were performed to determine the Pt content depth profile in the AAO templates. Figure 5 shows a typical RBS spectrum of a plasma electrode after 5 min Pt deposition time. The left side of the spectrum corresponds to AAO membranes

substrate contributions, whereas on the right side, the asymmetrical peak originates from α particles scattered by Pt atoms. The area under this Pt peak is directly related to the number of platinum atoms deposited on both surface and in the pores. The tail on the left side of the Pt peak indicates that the Pt atoms have diffused into AAO pores. Moreover, it is possible to deduce the Pt depth profile from this spectrum. By fitting the experimental spectrum with a simulated spectrum (using SIMNRA software) the depth profile can be recovered by an iteration process until the simulated spectrum matches the experimental spectrum.

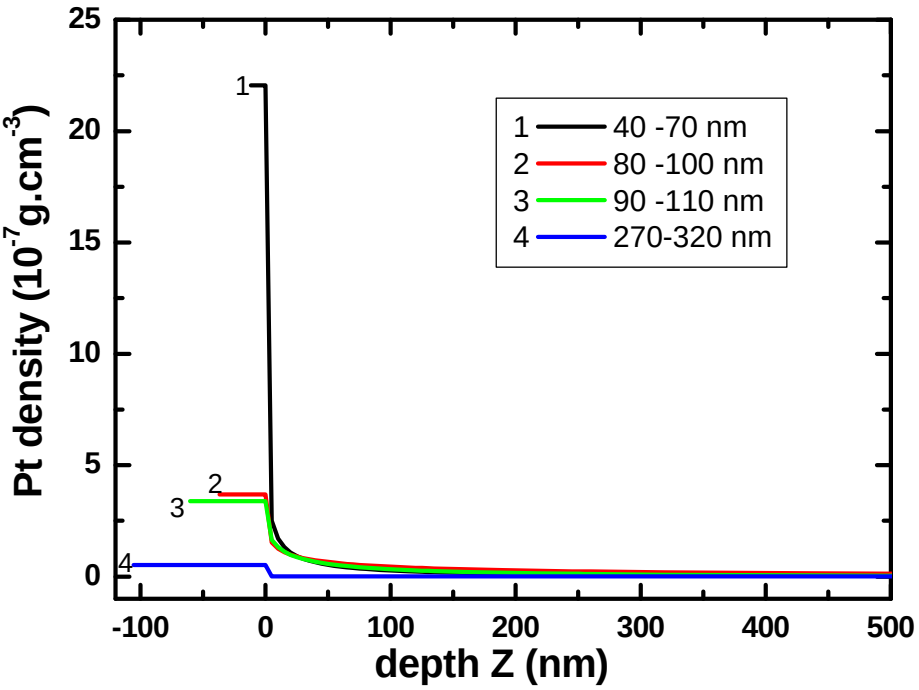

Figure 6: The density depth profile of Pt

We observed that the resulting depth profile is similar as Pt depth profile in porous carbon layer [1,2]: a growing layer above the porous medium, with the constant density Z1(t) and the mean thickness h (t) = z_0(t) (z<0); a diffusion layer in the porous medium, which extends in the z > 0 domain; and the interface between the growing layer and porous media, where the density profile is continuous (z=0). In porous layer, the Pt depth profile corresponds to the known solution of anomalous diffusion processes that can be defined by Eq .1 [1]. Hence, we still use this equation to define the diffusion

process in AAO channels and fit the depth profile with different pore size.

$\rho(z,t) = Z_1(t), \quad -z_0 < z \leq 0$

$\rho(z,t) = Z_1(t)\exp[-z^{2+\theta}/Z_2(t)] \quad z > 0$

θ is the dimensionless coefficient which characterizes the anomalous diffusion behaviour. If $\theta<0$ then the behaviour is superdiffusive else if $\theta>0$ it is subdiffusive. The deduced depth profiles of Pt deposited on the template, with different pore size, are displayed in Figure 6. The density on the surface is decreasing, but the thickness is increasing as the pore size increasing. The best fits correspond to θ changing between -1.76 to -1.6, which means that Ar plasma exposure during Pt deposition induces superdiffusion and the diffusion rate is different in different pore size. When the pore size increasing from 40 to 320 nm, the density on the surface is lowered from 23 $\mu g.cm^{-2}$ to 5 $\mu g.cm^{-2}$ and the maximum reached depth of Pt is from 2 μm to 20 μm. Pt atoms diffused more efficiently into the pores with largest size, which is consistent with the results from SEM. So combined SEM, EDX and RBS measurements suggest that Pt atoms arriving with a relatively high kinetic energy [6] undergo multiple scattering and diffusion on the surface of the inner walls of AAO ending by cluster growth.

Conclusions

In conclusion, the morphology and depth concentration profile of sputtered Pt atoms into porous AAO templates has been observed. The pore size is decreasing as the Pt is deposited. The morphology of the surface has a dramatically effect on the transport process in the pores. So, a concentration gradient extended as deep as 20 μm into the diffusion layer, depending on the pore size. Pt clusters are evidenced along the pore walls as resulting from transport/diffusion/adsorption/clustering process.

Reference

1. P. Brault, C. Josserand, J. Bauchire, A. Caillard, C. Charles, and R.W. Boswell, Phys. Rev. Lett. 102 (2009) 045901.
2. A. Caillard, P. Brault, J. Mathias, C. Charles, R. W. Boswell and T. Sauvage, Surf. Coat. Technol. 200, (2005) 391.
3. A. Caillard, C. Charles, R. Boswell and P. Brault, J. Phys. D: Appl. Phys. 41 (2008) 185307.
4. A. Caillard, C. Charles, R. Boswell, A. Meige and P. Brault, Plasma Sources Sci. Technol. 17 (2008) 035028

5. H. Rabat, C. Andreazza, P. Brault, A. Caillard, F. Beguin, C. Charles, R. Boswell,Carbon.47 (2009) 209
6. P. Brault, A. Caillard, A. L. Thomann, J. Mathias, C. Charles, R. W. Boswell, S. Escribano, J. Durand and T. Sauvage, J. Phys. D. 34 (2004)3419.
7. A. T. Haug, R. E. White, J. W. Weidner, W. Huang, S. Shi, N. Rana, S. Grunow and T. Stoner. J. Electrochem. Soc. 149 (2002) A868.
8. T. H. Yang, Y. G. Yoon, C. S. Kim, S. H. Kwak and K. H. Yoon, J. Power Sources. 106 (2002) 328.
9. S. Hira, J. Kim and S. Srinivasan, Electrochem. Acta. 42(1997) 1587
10. H. Masuda, H. Yamada, M. Satoh, and H. Asoh, M. Nakao and T. Tamamura, Appl. Phys. Lett. 71 (1997) 2770.
11. H. Masuda and K. Fukuda, Science. 268 (1995) 1466 .
12. M. Saito, M. Kirihara, T. Taniguchi, and M. Miyagi, Appl. Phys. Lett. 55 (1994) 607 .
13. K.W. Lux, K.J.Rodriguez, Nano Lett. 6. No.2 (2006) 288.
14. J. Shui, J.C.M. Li, Nano Lett.9.No.4 (2009) 1307.
15. B. D. Yao, D. Fleming, M. A. Morris, S. E. Lawrence, Chem. Mater. 16 (2004) 4851.
16. L. Li, Y. Zhang, G. Li , L.D Zhang, Chem. Phys. Lett. 378 (2003) 244.
17. Q. Wang, X. Sun, S. Luo, L. Sun, X. Wu, M. Cao, and C. Hu, Crystal Growth & Design. 7 (2007) 2667.
18. Y. Wang, J. Y. Lee, H. C. Zeng, Chem. Mater. 17 (2005) 3899.
19. C. Shi, G. Wang, N. Zhao, X. Du, J. Li, Chem. Phys. Lett. 454 (2008) 75
20. X. X. Li, F. Y. Cheng, B. Guo, J. J. Chen, Phys. Chem. B. 109 (2005) 14017.
21. K.T. Huang, P.C. Kuo, Y.D. Yao, Thin Solid Films 517 (2009) 3243